JOURNAL OF NANO- AND ELECTRONIC PHYSICS
Vol. **14** No 2, 02017(4pp) (2022)

ЖУРНАЛ НАНО- ТА ЕЛЕКТРОННОЇ ФІЗИКИ
Том **14** № 2, 02017(4cc) (2022)

Electrical Properties of a Nanosynthesized PGDC Electrolyte Material

Somoju Ramesh*

Department of Physics, School of Science, GITAM (Deemed to be University), 502329 Telangana, India

(Received 01 February 2022; revised manuscript received 18 April 2022; published online 29 April 2022)

Pr-Gd doped ceria nanopowder particles of the PGDC ($Ce_{0.8}Gd_{0.18}Pr_{0.02}O_{2-\delta}$) sample were synthesized by a sol-gel process modified using sucrose and pectin. XRD results showed $Fm\bar{3}m$ space group and a cubic structure. The average crystallite size was in the range of 9-13 nm. The average crystallite size value increased with temperature. Raman spectra showed more oxygen vacancies than undoped ceria. The relative density of the sample was 97 %. SEM images clearly showed a denser surface with grains. The electrical conductivity of the PGDC sample was 0.01461 S/cm at 700 °C with an activation energy of 0.92 eV.

Keywords: Modified sol-gel process, XRD, SEM, Raman, Electrical conductivity.

DOI: 10.21272/jnep.14(2).02017 PACS numbers: 81.20.Ka, 81.07.Wx, 61.05.cp, 78.30.j, 72.80.Ng, 82.47.Ed

1. INTRODUCTION

Electrolyte materials are essential among other cell components in solid oxide fuel cells (SOFCs) [1-3]. Traditional/commercial electrolyte materials (yttrium, scandium stabilized zirconia, bismuth-based) operate over higher temperatures (greater than 1000 °C) [4-7]. Doped ceria materials are alternate electrolytes at lower operating temperatures (600-800 °C). The electrolyte should be of high density and higher electrical conductivity. However, the electrical conductivity of doped ceria depends on proper doping concentrations [1, 4, 8, 9].

The synthesis process plays a significant role in the production of nanosized powder particles. The main objective of the present study is to synthesize nanoparticles more effectively than the existing methods like solid-state reaction, ball milling, sol-gel process, precipitation methods, and to prepare a dense ceramic electrolyte (more than 95 %) at relatively low sintering temperatures (lower than 1300 °C). Higher sintering temperatures result in micro-cracks, incompatibility across the cell components, chemical instability, etc.

The composition of PGDC ($Ce_{0.8}Gd_{0.18}Pr_{0.02}O_{2-\delta}$) nanopowder particles was synthesized by a sol-gel process modified using sucrose-pectin [10, 11]. In the conventional sol-gel process, chemicals such as ethylene glycol and ammonium nitrate were used. Ethylene glycol and ammonium nitrate chemicals were treated as environmental pollutants. The sol-gel process modified using sucrose-pectin is cost-effective and environmentally friendly. Suci [10] reported first-time sol-gel process modification with sucrose-pectin to synthesize high purity, uniform size nanoparticles.

The present study focuses on synthesis and characterization using XRD, SEM, Raman spectrometer, and ac impedance meter of PGDC sample.

2. EXPERIMENTAL

The PGDC ($Ce_{0.8}Gd_{0.18}Pr_{0.02}O_{2-\delta}$) sample was prepared through the sol-gel process modified using sucrose and pectin as chelating agents. (Finar made) cerium nitrate, gadolinium nitrate, and praseodymium nitrate pure materials were used as starting materials. As per the stoichiometry, praseodymium, gadolinium, and cerium nitrates were calculated and weighed accurately. Commercial grade sucrose and pectin materials were used for gel preparation and mixed in mass ratio sucrose: pectin = 30 : 1. Synthesis details can be found elsewhere [10, 11].

Synthesized powders were calcined at 600 °C and then pressed into circular pellets (10 mm × 2 mm). Then pellets were sintered in air at 1250 °C for 6 h. The densities of the sintered samples were measured using the Archimedes method. Powder XRD patterns were recorded using PANalytical X'Pert Pro. SEM images were taken with ZEISS Sigma. LABRAM-HR was used to record the Raman spectra. HIOKI 3531Z LCR meter was used to record the sample resistance in the frequency range 42-5 MHz, in the temperature range 350-700 °C.

3. RESULTS AND DISCUSSION

3.1 Structural Characterization

Fig. 1 shows X-ray diffraction patterns of the PGDC sample at different temperatures. The sample shows a single phase with space group $Fm\bar{3}m$ (JCPDS reference), and a cubic structure. The crystallite size (D_{XRD}) was calculated using the Scherrer equation:

$$D_{XRD} = 0.9\lambda/\beta\cos\theta, \quad (1)$$

where λ is the wavelength of the radiation, θ is the diffraction angle, β is the full width at half maximum.

It is noticed that XRD peaks with higher FWHM at room temperature and 600 °C indicate a small average crystallite size (calculated using Eq. (1)), and the sizes are in the range 9-13 nm. The modified sol-gel method results in finer size particles [10, 11]. Furthermore, the powder XRD pattern at 1250 °C has shown an average crystallite size of 45 nm. The average crystallite size increased with temperature. Pr and Gd dopants introduced into Ce lead to a peak shift towards lower dif-

* ramesh.ou1@gmail.com

fraction angles. Due to this, there is a change in the lattice parameter. The lattice parameter (5.416 Å) was calculated using formula

$$a = d\sqrt{h^2 + k^2 + l^2}\,, \qquad (2)$$

where a is the lattice parameter, d is the lattice spacing and (h,k,l) are the Miller indices.

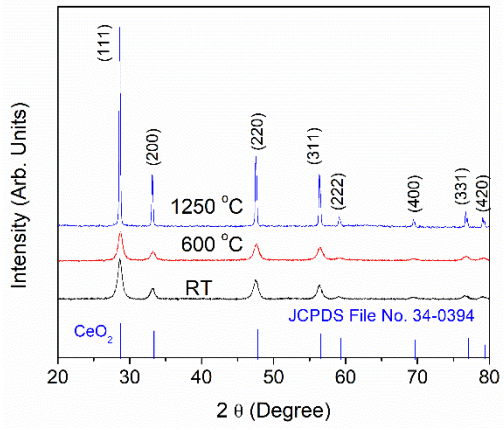

Fig. 1 – XRD patterns of the PGDC powder samples at different temperatures

3.2 Relative Density

Fig. 2 shows the relative density of the PGDC sample. Fig. 2 shows that the Pr- and Gd-doped ceria samples' relative density varies with temperature, i.e., relative density increases with temperature. Relative density was calculated using Eq. (3);

$$\text{Relative density } (D_{\text{rel.}}) = d_{\text{exp}}/d_{\text{theor.}} \qquad (3)$$

Theoretical density was calculated using the formula:

$$\text{Density } (\rho) = (n \cdot M)/(a^3 N_A), \qquad (4)$$

where n is the effective number of atoms, M is the atomic mass (in g), N_A is the Avogadro number (6.023×10^{23}/mole), a is the lattice constant (Å).

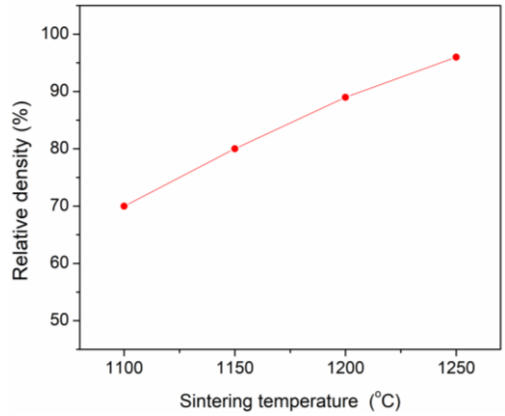

Fig. 2 – Relative density of the PGDC sample

3.3 Morphological Characterization

Fig. 3 a-c shows the SEM images of the PGDC sample at different temperatures. Fig. 3a presents the sample image at 600 °C, and it is clear that the surface shows a sponge-type porous material. Fig. 3b shows the sample at 1100 °C. Fig. 3c presents the sample with a high-density surface almost free from pores. These results are in good agreement with the relative density. Fig. 3d shows the dispersive energy spectra (EDS) of the sample; the elements Pr, Gd, Ce are present as per the composition.

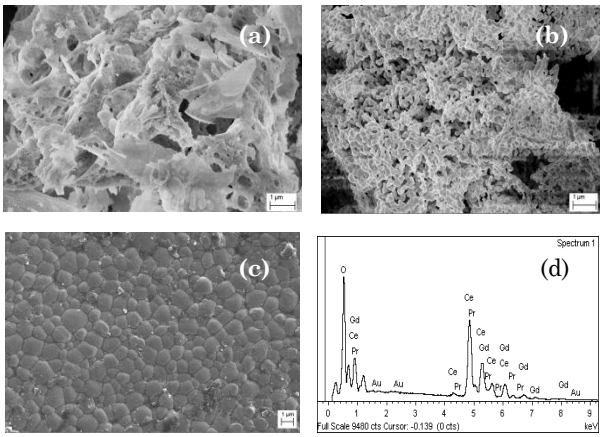

Fig. 3 – SEM images of the PGDC sample at (a) 600 °C, (b) 1000 °C, (c) 1250 °C, and (d) EDS

3.4 Raman Spectroscopy

The Raman spectra of the PGDC sample are shown in Fig. 4. Undoped ceria shows one band at 462.78 cm^{-1}, whereas Pr-Gd doped ceria exhibits two bands at 461 cm^{-1} and 577 cm^{-1}. It is worthy to note that the extra band is present at 577 cm^{-1} compared to undoped ceria. It indicates higher oxygen vacancy concentration for the PGDC sample [12, 13]. Furthermore, there is a decrease in intensity and a peak shift towards the lower frequency region. The peak shift is due to the ionic radius difference between host and dopants (Gd^{3+}(1.05 Å), Pr^{3+}(1.126 Å), and Ce^{4+}(0.97Å)).

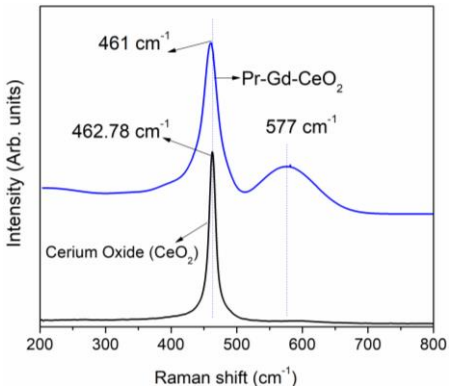

Fig. 4 – Raman spectra of the PGDC sample

3.5 Electrical Conductivity

Fig. 5 shows the electrical conductivity versus frequency at different temperatures of the PGDC sample. It can be seen at lower frequencies that the conductivity is almost constant and increases at higher frequencies. The electrical conductivity values were calculated using the following equation:

$$\sigma = L/RA, \quad (5)$$

where R is the total resistance measured by the impedance meter, L is the thickness, A is the cross-sectional area of the sample.

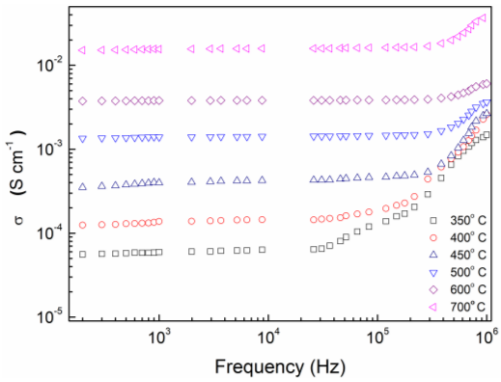

Fig. 5 – Electrical conductivity versus frequency of the PGDC sample

Fig. 6 shows the electrical conductivity versus 1000/T of the PGDC sample. It can be seen that the curves follow the Arrhenius nature. The activation energy was calculated by linear fitting of the curves from Fig. 6. The activation energy was calculated using eq. (5), and it is 0.92 eV. The lower frequency intercept values from Fig. 5 were taken as conductivity values.

$$\sigma = \frac{\sigma_0}{T}\exp\left(-\frac{E_a}{kT}\right). \quad (6)$$

The electrical conductivity increased due to the increase in oxygen vacancies (V^{oo}_O). Gd^{3+} and Pr^{3+} dopants form defects with host material ceria, resulting in a higher oxygen vacancy concentration (V^{oo}_O). According to the Kroger-Vink notation [14, 15]:

$$M_2O_3 \xrightarrow{2CeO_2} 2M'_{Ce} + 3O^x_O + V^{oo}_O, \quad (7)$$

where M = Gd or Pr, (V^{oo}_O) = oxygen vacancy concentration, Gd'$_{Ce}$ or Pr'$_{Ce}$ = Gd^{3+} or Pr^{3+} doped into host Ce^{4+} .

Due to V^{oo}_O, oxygen vacancy occupancy in the fluorite structure re-orientation process takes place. V^{oo}_O oxygen vacancy forms defect associate pairs with dopant cations (Gd'$_{Ce}$. V^{oo}_O, Pr'$_{Ce}$. V^{oo}_O) or (Gd'$_{Ce}$. V^{oo}_O. Gd'$_{Ce}$, Pr'$_{Ce}$. V^{oo}_O. Pr'$_{Ce}$) [14, 15].

The PGDC sample exhibits improved conductivity (0.01461 S/cm) with activation energy (0.92 eV). These values are compared with those reported in the literature [13-17].

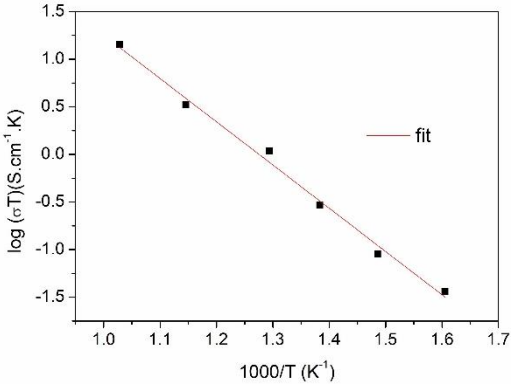

Fig. 6 – Electrical conductivity versus 1000/T of the PGDC sample

4. CONCLUSIONS

The PGDC sample was successfully synthesized through a sol-gel process modified using sucrose-pectin. The average crystallite size was in the range of 9-13 nm. High-dense ceramic material was prepared by sintering at 1250 °C for 6 h. The lattice parameter of the PGDC sample was 5.416 Å, and it is higher than that of undoped ceria (5.409 Å). The sample exhibited a single phase with a cubic structure. The Raman spectra showed more oxygen vacancies for Pr-Gd doped ceria than for undoped ceria. The morphology of the samples showed a dense surface with grains clearly. The electrical conductivity of the PGDC sample was 0.01461 S/cm, with an activation energy of 0.92 eV.

REFERENCES

1. N.Q. Minh, T. Takahashi, *Science and Technology of Ceramic Fuel Cells* (Netherlands: Elsevier publications: 1995).
2. H. Inaba, H. Tagawa, *Solid State Ion.* **83**, 1 (1996).
3. Larmine dicks, *Fuel Cell Systems Explained* (London: John Wiley & Sons: 2000).
4. B.C.H. Steele, *Solid State Ions* **129**, 95 (2000).
5. J.A. Kilner, *Solid State Ions* **129**, 13 (2000).
6. J. Neilsen, A. Hagen, Y.L. Liu, *Solid State Ions* **181**, 517 (2010).
7. N. Kim, B.H. Kim, D. Lee, *J. Power Source.* **90**, 139 (2000).
8. F.Y. Wang, S. Chen, Q. Wang, S. Yu, S. Cheng, *Catal. Today* **97**, 189 (2004).
9. F.Y. Wang, B.Z. Wan, S. Cheng, *J. Solid State Electrochem.* **9**, 168 (2005).
10. C. Suciu, L. Gagea, A.C. Hoffmann, M. Mocean, *Chem. Eng. Sci.* **61**, 7831 (2006).
11. Z. Wang, G.M. Kale, M. Ghadiri, *J. Mater. Chem.* **21**, 6494 (2011).
12. W.H. Weber, K.C. Hass, J.R. McBride, *Phys. Rev. B* **48**, 178 (1993).
13. K. Venkataramana, C. Madhuri, Ch. Madhusudan, Y. Suresh Reddy, C. Vishnuvardhan Reddy, *J. Appl. Phys.* **126**, 144901 (2019).
14. L. Spiridigliozzia, G. Dell'Aglia, G. Accardoc, S.P. Yoon, D. Frattini, *Ceram. Int.* **45**, 4570 (2019).
15. Anirban, A. Dutta, *Solid State Ions* **295**, 48 (2016).
16. Aliya Arabaci, *Open Chem.* **16**, 827 (2018).
17. Y. Liu, L. Fan, Y. Cai, W. Zhang, B. Wang, B. Zhu, *Appl. Mater. Interface.* **9**, 23614 (2017).

Електричні властивості наносинтезованого електролітного матеріалу PGDC

Somoju Ramesh

Department of Physics, School of Science, GITAM (Deemed to be University), 502329 Telangana, India

Частинки нанопорошку церію, доповані Pr-Gd, зразка PGDC ($Ce_{0.8}Gd_{0.18}Pr_{0.02}O_{2-\delta}$) синтезовано золь-гель процесом, модифікованим із застосуванням сахарози та пектину. Результати XRD показали просторову групу $Fm\bar{3}m$ та кубічну структуру. Середній розмір кристалітів був у межах 9-13 нм. Середнє значення розміру кристалітів збільшувалося з підвищенням температури. Раманівські спектри показали більше вакансій кисню для легованих зразків, ніж для нелегованих церієм. Відносна густина зразка становила 97 %. Зображення SEM чітко показали поверхню із більш щільно розташованими зернами. Електропровідність зразка PGDC становила 0,01461 См/см при 700 °C з енергією активації 0,92 еВ.

Ключові слова: Модифікований золь-гель процес, XRD, SEM, Раманівські спектри, Електропровідність.